Mazaheri, Hesam; Saber, Hossein; Fattaheian-Dehkordi, Sajjad; Moeini-Aghtaie, Moein;
Fotuhi-Firuzabad, Mahmud; Lehtonen, Matti

Harnessing power system flexibility under multiple uncertainties

Harnessing power system flexibility under multiple uncertainties

Hesam Mazaheri[1] | Hossein Saber[2] | Sajjad Fattaheian-Dehkordi[2,4] |
Moein Moeini-Aghtaie[3] | Mahmud Fotuhi-Firuzabad[2] | Matti Lehtonen[4]

[1]Department of Electrical and Computer Engineering, Texas A&M University, College Station, Texas, USA

[2]Department of Electrical Engineering, Sharif University of Technology, Tehran, Iran

[3]Department of Energy Engineering, Sharif University of Technology, Tehran, Iran

[4]Department of Electrical Engineering and Automation, Aalto University, Espoo, Finland

Correspondence

Mahmud Fotuhi-Firuzabad, Department of Electrical Engineering, Sharif University of Technology, Tehran 11365-11155, Iran.
Email: fotuhi@sharif.edu

Abstract

Increasing the intermittent outputs of renewable energy sources (RESs) has forced planners to define a new concept named flexibility. In this regard, some short- and long-term solutions, such as transmission expansion planning (TEP) and energy storage systems (ESSs) have been suggested to improve the flexibility amount. A proper optimization procedure is required to choose an optimal solution to improve flexibility. Therefore, a mixed-integer linear programming (MILP) direct-optimization TEP versus ESSs co-planning model is presented in this paper to enhance power system flexibility. In doing so, a novel RES-BESS-based grid-scale system flexibility metric is proposed to investigate the improvement of flexibility amount via ESSs modules in the numerical structure. In this paper, a novel repetitive fast offline method has been proposed to quickly reach the desired amount of flexibility by defining an engineering price/benefit trade-off to finally find the best investment plan. Also, multiple uncertainties associated with wind farms and demanded loads and a practical module-type battery energy storage system (BESS) structure for each node are defined. The proposed model is applied to the modified IEEE 73-bus test system including wind farms, where the numerical results prove the model efficiency as BESS impacts on flexibility, investment plans and power system economics.

1 | INTRODUCTION

In recent years, the integration of renewable energy sources (RESs) has significantly as well as rapidly increased in the power systems generation sectors [1, 2]. The proliferation of RESs with their intermittent generation outputs has demanded a higher degree of operational system flexibility [3–5]. To cope with the intermittency of RESs' outputs and achieve a higher level of system flexibility, power system investors and planners have tried to suggest short- and long-term solutions [3, 6]. Amongst, expanding the transmission capacity, called transmission expansion planning (TEP) [7] and employing energy storage systems (ESSs) [8, 9] have been introduced as the pivotal solutions. Due to the required considerable capital investment cost in the expansion of TEP and ESSs, developing a proper optimization procedure to determine the optimal capacity/location of trans-

mission lines and ESSs modules would be essential considering the adequate uncertainties [10, 11].

As a comparison between high-capacity applicable ESSs in transmission level such as battery energy storage systems (BESS), pumped hydro energy storage (PHES), and compressed air energy storage (CAES), BESS are more practical because, unlike periodicals, they can be applied in distributed capacity which helps plan to add the desired amount of capacity in each transmission network. Also, BESS has lower construction costs, as the price of these distributed modules has been more affordable in recent years, with no geographical constraints compared to PHES and CAES. Moreover, BESS integration has been more efficient with operational benefits in RES-based power grids than in CAES, which is more practical in thermal generator grids. Therefore, impressive progress in BESS modules can be a promising solution to considerably address

the new challenges in power system flexibility and economics [3, 12, 13].

Since ESSs and TEP have mutual impacts on each periodical, the expansion of ESSs modules has been extensively studied in modern power systems. Authors in [14] try to introduce a robust ESSs framework to alleviate the fluctuating generation of RESs based on a non-convex non-linear AC optimal power flow method, while reference [15] investigates an optimal transmission network reconfiguration model considering non-linear AC power flow. In [8], a multi-period optimal power system operation is presented considering the non-linear ESSs and AC power flow models. Authors in [16] develop a tri-level model to simultaneously determine the optimal sizing and siting of merchant BESS and TEP to maximize the BESS owners' profit and minimize the cost of TEP decisions. Reference [17] proposes a two-stage robust model for BESS and TEP co-planning considering RESs uncertainty. In [18], sizing/siting optimization of BESS models has been optimally defined for reducing reverse power flow and minimizing total system losses. Reference [19] presents an investment model in active distribution networks to determine the selection of type, capacity, and location of BESS considering uncertainties. Authors in [20] suggest a co-planning TEP and BESS expansion model in a market-driven environment to maximize social welfare. A metaheuristic optimization model for RESs optimal planning is proposed in [2] to minimize BESS's total power and energy losses. In [21], a stochastic, multi-stage, co-planning optimization model of transmission and BESS expansion is presented to enhance power system flexibility in dealing with system uncertainties. Finally, authors in [22] suggest a multi-stage mixed-integer linear programming (MILP) model including transmission as well as BESS planning under long-term uncertainties to improve power system flexibility.

Furthermore, power system planners have measured the system flexibility in several studies as a capacity to employ flexible resources and satisfy the specific range of uncertainties in long-term power grid planning and real-time operation. In [23], a robust optimization model is defined to measure the long-term planning and short-term operation metrics of flexibility. Authors in [24] suggest an adaptive robust optimization system flexibility model under a unit commitment time-scale framework considering wind uncertainty. In [25], a long-term stochastic co-optimization planning model is presented to minimize total cost and maintain power system flexibility under RESs uncertainties. A flexibility evaluation method in distribution networks has been presented in [26] based on the feasibility analysis of uncertain regions of solar photovoltaic generations and demands. Authors in [27] try to propose a set of optimization problems based on the optimal power flow concept to estimate the flexibility at the boundary nodes of distribution and transmission systems. In [28], a hydro-photovoltaic-pumped storage generation expansion planning is proposed considering solar and load uncertainty to balance planning costs and operational flexibility constraints. Reference [29] tries to propose a flexibility framework for distributed energy resources considering the capacity, ramp, duration, and cost as flexibility metrics. Finally, an analytical framework for estimating the operational

flexibility of distribution networks is defined in [30] including the quantification of node flexibility, the system flexibility matching, and the transmission system flexibility.

According to the literature mentioned above, some studies have presented the planning of non-linear ESSs, while Periodicals have tried to model an operational scheme considering ESSs and non-linear AC optimal power flow. In these references, the linearization method has not been studied; also, most of them have presented the AC scheme for distribution level, as expected, to design the exact details of these grids. Moreover, some studies have proposed the co-planning of TEP and ESSs considering RESs uncertainty to improve power system economics, while periodicals have tried to present flexibility metrics in long-term planning and real-time operation. Finally, some have tried to present optimal power flow to estimate the operational flexibility constraints for distributed energy resources. In these references, improvements in power grid flexibility were not the primary goal and although authors in [3, 31] have tried to present some metrics to measure system flexibility, in recent research works, none has studied numerical flexibility metrics in TEP versus BESS modules planning under RESs uncertainties in which system flexibility has been measured as well as improved integrating BESS modules in which a repetitive offline method has been applied with a fast-converged optimization model to reach the desired amount of system flexibility in an RES-based power system.

In this regard, an MILP direct-optimization co-planning model is presented in this paper to model power system flexibility. In this regard, the stochastic co-planning model of TEP versus BESS modules has been proposed to improve power system flexibility, specifically by integrating BESS modules in the network. In doing so, a novel RES-BESS-based grid-scale system flexibility metric is proposed to hopefully assess the numerical improvement of the system flexibility by BESS modules. It should be noted that a new repetitive offline method has been defined to reach the desired amount of system flexibility in each network. This method suggests an engineering price/benefit trade-off to find the best investment plan in terms of flexibility concept. Furthermore, multiple uncertainties associated with wind farms generation as well as demands have been considered, while a practical module-type distributed BESS structure for each node is measured. One of the important contributions of this paper is to apply a new fast solution method to reach the desired amount of flexibility target. As a result, the contributions of this paper are as follows:

- A novel RES-BESS-based grid-scale system flexibility metric is presented to optimally measure as well as improve system flexibility by integrating BESS modules in an RES-based power system. To do so, a MILP stochastic co-planning direct-optimization formulation is modelled to solve the proposed model by converting two-stage optimization into one-stage with an efficient linearization method in which the model is converged faster.
- A new repetitive offline fast solution method is defined to reach the desired amount of system flexibility. In this mechanism, a system flexibility target based on the

investment budget is considered to define a price/benefit trade-off, which helps to finally find the best investment plan. As an explanation, this method has been applied to converge the programming faster. However, by applying multi-objective optimization methods in which the flexibility index will be solved in the programming, the model would converge slower, even unsolvable in a huge power system network. Therefore, we have defined this approach to reach the desired flexibility amount.

- A practical module-type distributed BESS structure is considered in a realistic power system case study as verification for our model. Although this model is presented to address problems previously in the TEP approach like constructing new transmission lines and economic issues, BESS modules' specific ability has been considered as the main reason to reach the desired power system flexibility. Therefore, trade-offs are discussed in TEP versus BESS modules to optimally prove the efficiency of BESS modules on RES-BESS-based grid-scale system flexibility, investment plans and power system economics under multiple uncertainties.

The remainder of this paper is presented as follows. Section 2 introduces the proposed method for multiple uncertainties scenarios. In Section 3, the mathematical formulation of the stochastic co-optimization model, including constraints, flexibility measurement, and the objective function, are presented. A flowchart of the proposed algorithm, a logic scheme, and a proper explanation of the solution methodology are presented in Section 4. The case study is discussed in Section 5 in which a grid-scale test system has been defined, while numerical results and discussion have been analysed. The concluding remarks are presented in Section 6. Finally, an Appendix is considered to present the linearization method as well as RESs and BESS data.

2 | MULTIPLE UNCERTAINTIES SCENARIOS

Due to the stochastic nature of multiple uncertainties in electric power systems, it is required to appropriately model the associated uncertainties in the operation and planning studies of power systems. To deal with the power system uncertainties in the previous research works, several different approaches have been utilized such as scenario-based stochastic programming and robust optimization approach. Amongst, the scenario-based stochastic method is one of the most applied methods in various researches [32–36]. Generally, wind speed uncertainty can be modelled using normal [37] or Weibull [2] probability distribution functions. Moreover, a multi-band uncertainty set of wind power has been defined to combine the probability distribution characteristics of wind and load prediction errors [6, 10].

In this study, the normal probability distribution function is applied to generate the associated scenarios of wind farms generation. In this regard, the mean and the standard deviation of the normal probability distribution function are determined using the curve fitting technique on historical data. In detail, after defining the mean and standard deviation values of uncertainty, many scenarios are generated using Monte Carlo simulation [19, 38]. Thus, in the generated scenarios, the wind farms generation at each hour is equal to the forecasted value at that hour plus an error, which is randomly generated based on the probability distribution. Since a large number of scenarios apply extra computational burden to the problem, a suitable scenario reduction method must be utilized. In this study, a well-known algorithm called the backward scenario reduction method is employed to reduce the number of generated scenarios [39]. Through this algorithm, at each iteration, the scenario with the least probability will be removed and its probability will be added to the closest scenario. This iterative procedure will continue until the pre-specified number of scenarios is determined. Finally, the resulting scenarios are fed into the proposed optimization problem.

3 | MATHEMATICAL MODEL

3.1 | Constraints

To measure the RES-BESS-based grid-scale system flexibility, the MILP model of TEP versus BESS co-planning is presented as follows. In this regard, the balance of generated and consumed power electricity is presented in (1). To clarify, power flow in available and installed transmission lines, generating units, wind farms generation and BESS modules discharging power are considered on the left side of this equation, while the right side presents demanded loads, BESS modules charging power, and wind farms spillage power. Due to the non-linearity of the planning of the power flow for installed transmission lines constraints, the well-known Big-M method is applied to linearize the DC optimal power flow formulations [40, 41]. The linearization method has been explained in Appendix A1. Therefore, the power flow for available transmission lines is presented in (2), while the linearized power flows for installed transmission lines are presented in (3)–(5). Finally, power flow and generating units limits are shown in (6)–(10).

It should be noted that the big number in the Big-M method is defined as ten times the maximum transmission lines capacity [42]. As a discussion in AC/DC power flow, it is worth mentioning that both have non-linear constraints in power system planning. However, the computational complexity for linearizing AC power flow is higher than DC power flow, which contradicts our fast-converged method. Moreover, the proposed model has been defined in transmission level in which the ratio of X to R is more significant than in distribution networks. As a result, using DC power flow can be more efficient at the transmission level with lower computational complexity, while the linearized AC power flow should be applied to measure system flexibility at the distribution level [43–45].

$$\Psi_{l,i}^L \left(F_{s,l,t} + F'_{s,l,t} + F''_{s,l,t} + F'''_{s,l,t} \right) + \Psi_{g,i}^G P_{s,g,t}^G + P_{s,i,t}^W + P_{s,i,t}^{B^-}$$

$$= P_{s,i,t}^D + P_{s,i,t}^{B^+} + P_{s,i,t}^{ws} : \quad \forall s \in S, l \in L, i \in N, g \in G, t \in T$$

$$\subseteq \left\{ Z^{L \times N}, Z^{G \times N}, R^{S \times L \times T}, R^{S \times G \times T}, R^{S \times N \times T} \right\} \quad (1)$$

$$F_{s,l,t} + \Psi^L_{l,i}\beta_l\Theta_{s,i,t} = 0 : \quad \forall s \in S, l \in L, i \in N, t \in T$$

$$\subseteq \left\{ R^L, Z^{L \times N}, R^{S \times L \times T}, R^{S \times N \times T} \right\} \tag{2}$$

$$-\Re(1-\alpha'_l) \le F'_{s,l,t} + \Psi^L_{l,i}\beta_l\Theta_{s,i,t} \le \Re(1-\alpha'_l) : \forall s \in S, l \in L,$$

$$i \in N, t \in T \subseteq \left\{ \{0,1\}^L, R^L, Z^{L \times N}, R^{S \times L \times T}, R^{S \times N \times T} \right\} \tag{3}$$

$$-\Re(1-\alpha''_l) \le F''_{s,l,t} + \Psi^L_{l,i}\beta_l\Theta_{s,i,t} \le \Re(1-\alpha''_l) : \forall s \in S, l \in L,$$

$$i \in N, t \in T \subseteq \left\{ \{0,1\}^L, R^L, Z^{L \times N}, R^{S \times L \times T}, R^{S \times N \times T} \right\} \tag{4}$$

$$-\Re(1-\alpha'''_l) \le F'''_{s,l,t} + \Psi^L_{l,i}\beta_l\Theta_{s,i,t} \le \Re(1-\alpha'''_l) : \quad \forall s \in S, l \in L,$$

$$i \in N, t \in T \subseteq \left\{ \{0,1\}^L, R^L, Z^{L \times N}, R^{S \times L \times T}, R^{S \times N \times T} \right\} \tag{5}$$

$$-P^L_{l,max} \le F_{s,l,t} \le P^L_{l,max} : \quad \forall s \in S, l \in L, t \in T \subseteq \left\{ R^L, R^{S \times L \times T} \right\} \tag{6}$$

$$-\alpha'_l P^L_{l,max} \le F'_{s,l,t} \le \alpha'_l P^L_{l,max} : \quad \forall s \in S, l \in L, t \in T$$

$$\subseteq \left\{ \{0,1\}^L, \ R^L, R^{S \times L \times T} \right\} \tag{7}$$

$$-\alpha''_l P^L_{l,max} \le F''_{s,l,t} \le \alpha''_l P^L_{l,max} : \quad \forall s \in S, l \in L, t \in T$$

$$\subseteq \left\{ \{0,1\}^L, \ R^L, R^{S \times L \times T} \right\} \tag{8}$$

$$-\alpha'''_l P^L_{l,max} \le F'''_{s,l,t} \le \alpha'''_l P^L_{l,max} : \quad \forall s \in S, l \in L, t \in T$$

$$\subseteq \left\{ \{0,1\}^L, \ R^L, R^{S \times L \times T} \right\} \tag{9}$$

$$P^G_{g,min} \le P^G_{s,g,t} \le P^G_{g,max} : \quad \forall s \in S, g \in G, t \in T \subseteq \left\{ R^G, R^{S \times G \times T} \right\} \tag{10}$$

The charging and discharging power limits of BESS modules are presented in (11), (12). Notice that the constraints related to binary variables of BESS charging and discharging statuses are not considered in this paper as operational variables depend on the efficiency of BESS modules. Therefore, they can be ignored in high-efficiency ESSs technologies (>90%) when charging or discharging modes have already been discovered [46, 47]. Constraint (13) tries to limit the number of installed BESS modules in each node, while wind farms' spillage power limit is presented in (14). Finally, BESS modules' state of charge (SoC) limit and BESS modules' SoC per hour are calculated in (15), (16) [13].

$$0 \le P^{B+}_{s,i,t} \le \delta^B_i P^B_{max} : \quad \forall s \in S, i \in N, t \in T \subseteq \left\{ Z^N, R^{S \times N \times T} \right\} \tag{11}$$

$$0 \le P^{B-}_{s,i,t} \le \delta^B_i P^B_{max} : \quad \forall s \in S, i \in N, t \in T \subseteq \left\{ Z^N, R^{S \times N \times T} \right\} \tag{12}$$

$$0 \le \delta^B_i \le \delta_{i,max} : \quad \forall i \in N \subseteq \left\{ Z^N \right\} \tag{13}$$

$$0 \le P^{ws}_{s,i,t} \le P^W_{s,i,t} : \forall s \in S, i \in N, t \in T \subseteq \left\{ R^{S \times N \times T} \right\} \tag{14}$$

$$0 \le E^B_{s,i,t} \le \delta^B_i E^B_{max} : \quad \forall s \in S, i \in N, t \in T \subseteq \left\{ Z^N, R^{S \times N \times T} \right\} \tag{15}$$

$$E^B_{s,i,t} = E^B_{s,i,t-1} + \eta P^{B+}_{s,i,t} - \eta^{-1} P^{B-}_{s,i,t} : \quad \forall s \in S, i \in N, t \in T \subseteq \left\{ R^{S \times N \times T} \right\} \tag{16}$$

3.2 | Flexibility measurement

A novel RES-BESS-based grid-scale system flexibility metric is defined to measure the power system flexibility numerically [3, 31]. In doing so, a new variable named maximum generating power is introduced in (17) including the maximum capacity of generating units and maximum wind farms generation. This variable normalizes the measurement of the system flexibility into a per-unit scale. Therefore, the novel flexibility index is defined in (18) at time t and node i under multiple uncertainties scenario s. It should be noted that the maximum generating power (17) is the similarity between TEP and ESSs in the grid flexibility concept, while the flexibility index (18) is the difference between TEP and ESSs models as the TEP model without ESSs has a simpler (18) equation in which the ESSs data will not be added. Therefore, the power systems will not properly be able to cope with daily variations in generated electricity powers and demanded loads as the flexibility concept which can prove the positive impacts of ESSs modules on power system flexibility.

In the proposed flexibility index, two sections are effectively considered to model the flexibility concept as the power systems' ability to cope with daily variations in generated electricity powers and demanded loads. The first section is defined to calculate the variation of generated powers minus consumed powers at any given time t and $t-1$. In doing so, we present variables $\{\Delta P^G_{s,g,t}, \Delta P^W_{s,i,t}, \Delta P^{B-}_{s,i,t}, \Delta P^{B+}_{s,i,t}, \Delta P^D_{s,i,t}\}$ by which the generated powers from generating units, wind farms, and BESS modules discharging power are subtracted from demanded loads and BESS modules charging power. In this regard, the flexibility bound is defined as the second section where the bound between the maximum and minimum capacity of generating units is added to maximum wind farms generation and installed BESS modules capacity. Note that generated powers from generating units, wind farms, and BESS modules discharging power are categorized into upward flexibility, while demanded loads and BESS modules charging power are defined as downward flexibility due to the fact that increasing the power grids generation with various sources is defined as upward flexibility and downward flexibility is a concept for decreasing the power grids generation.

As can be seen, the presented two sections in the flexibility index have equivalent influence on the definitive amount of the system flexibility. To clarify, the power variations including the difference at given time t and $t-1$ (1st section) have independently improved the system flexibility in an hourly manner as same as the flexibility bound including the maximum generation

in the system (2nd section) in a daily manner. As a result, the defined weight signals are considered to normalize the flexibility index in which the whole equation is divided to the maximum generating power to calculate the per-unit scale of the flexibility index as discussed previously. Notice that the minimum desirable amount of the system flexibility in the per-unit scale is considered 0.5 [31], which can be defined as the proposed weight signals. The RES-BESS-based grid-scale system flexibility obtained from (17) and (18) is calculated in (19). This model has applied the weighted sum of the flexibility index at node i.

$$P_{i,max} = \Psi_{g,i}^G P_{g,max}^G + P_{i,max}^W : \quad \forall i \in N, g \in G \subseteq \{R^N, R^G, Z^{G \times N}\} \tag{17}$$

$$\gamma_{s,i,t} = \left[\pi_1 \left(\Psi_{g,i}^G \Delta P_{s,g,t}^G + \Delta P_{s,i,t}^W + \Delta P_{s,i,t}^{B-} - \Delta P_{s,i,t}^{B+} - \Delta P_{s,i,t}^D \right) \right.$$
$$\left. + \pi_2 \left(P_{i,max} - \Psi_{g,i}^G P_{g,min}^G + \delta_i^B P_{max}^B \right) \right] \left(P_{i,max} \right)^{-1} : \forall s \in S, i \in N,$$
$$g \in G, t \in T \subseteq \{Z^N, R^N, R^G, Z^{G \times N}, R^{S \times G \times T}, R^{S \times N \times T}\} \tag{18}$$

$$\sigma : \quad min \left(X \mid \forall s \in S, t \in T \subseteq \{R^N, R^{S \times N \times T}\} \right), when :$$

$$X = \left(\sum_{i \in N} P_{i,max} \right)^{-1} \left(\sum_{i \in N} \gamma_{s,i,t} P_{i,max} \right) \tag{19}$$

$$\sigma_{min} \leq \sigma \tag{20}$$

Note that we calculate the minimum value of the system flexibility at time t on each scenario s as a reference of system flexibility measurement within the worst-case scenarios. Finally, a new offline fast method is suggested to repetitively improve the RES-BESS-based grid-scale system flexibility by defining the system flexibility target. In the proposed mechanism, the actual value of the RES-BESS-based grid-scale system flexibility in (19) is considered to satisfy the target presented in (20). The solution techniques have been expanded by a fast offline method to repetitively reach the desired amount of flexibility, combined with a fast-converged direct-optimization co-planning model. This model has been solved in the lowest computational time which is helpful in large-scale power systems. Therefore, an engineering price/benefit trade-off can be defined to finally find the best investment plan. Details of this offline method and also a conservative value for the target of the system flexibility are thoroughly explained in the methodology section.

3.3 | Objective function

The proposed objective function is presented in (21). The total cost including investment cost, operational cost, and interest rate as well as the lifetime of the planning problem is presented in (22). It should be noted that interest rate and lifetime of planning problem are defined to annualize the scale of long-term investment sub-problem with operational sub-problem. The total investment cost (23) includes the invest-

ment cost of newly installed transmission lines (25) and BESS modules (26). The total operational cost is presented in (24), which includes the operational cost of the generating units (27), the BESS modules (28) with the fixed as well as variable maintenance costs, and wind curtailment cost (29). Note that $\{\alpha'_l / \alpha''_l / \alpha'''_l, \delta_i^B, P_{s,g,t}^G, \gamma_{s,i,t}, \sigma\}$ are considered as the set of decision variables in the proposed framework.

$$O.F. : min \left(TC \mid \forall \omega \in \Omega, s \in S, l \in L, i \in N, g \in G, t \in T \right.$$
$$\left. \subseteq \left\{ \{0,1\}^L, Z^N, R^S, R^L, R^G, R^{S \times G \times T}, R^{S \times N \times T} \right\} \right) \tag{21}$$

$$TC = (1 + x)^{1-y} IC + OC \tag{22}$$

$$IC = IC^L + IC^B \tag{23}$$

$$OC = OC^G + OC^B + SC^W \tag{24}$$

$$IC^L = \sum_{l \in L} C_l^L \left(\alpha'_l + \alpha''_l + \alpha'''_l \right) \tag{25}$$

$$IC^B = \sum_{i \in N} \delta_i^B \left(C^B P_{max}^B + \hat{C}^B E_{max}^B \right) \tag{26}$$

$$OC^G = \sum_{\omega \in \Omega} \sum_{s \in S} \sum_{g \in G} \sum_{t \in T} \omega \rho_s C_g^G P_{s,g,t}^G \tag{27}$$

$$OC^B = \sum_{\omega \in \Omega} \sum_{s \in S} \sum_{i \in N} \sum_{t \in T} \omega \rho_s \left(\left(C^F \delta_i^B P_{max}^B \right) + C^V \left(P_{s,i,t}^{B+} + P_{s,i,t}^{B-} \right) \right) \tag{28}$$

$$SC^W = \sum_{\omega \in \Omega} \sum_{s \in S} \sum_{i \in N} \sum_{t \in T} \omega \rho_s C^W P_{s,i,t}^{ws} \tag{29}$$

s. t.:
(1)–(20) if linearized as an MILP
(1), (2), (A1)–(A3), (6)–(20) else as an MINLP

4 | SOLUTION METHODOLOGY

In this paper, the proposed framework is settled to consider the minimization of investment as well as operational costs emanated from newly installed transmission lines and BESS modules considering the system flexibility target. A detailed flowchart of the proposed framework is presented in Figure 1. In detail, the first loop is shown to consider generated uncertainties and constraints of the linearized model of the TEP vs. BESS modules framework. In this vein, all generated multiple uncertainties scenarios are modelled into the constraints to minimize the total cost. Then, in the second loop, the normal bi-level model of this stochastic co-planning problem is deferred into a single-step MILP model by the proposed linearization approach to efficiently release the computational burden of the problem. In this regard, the best investment option including
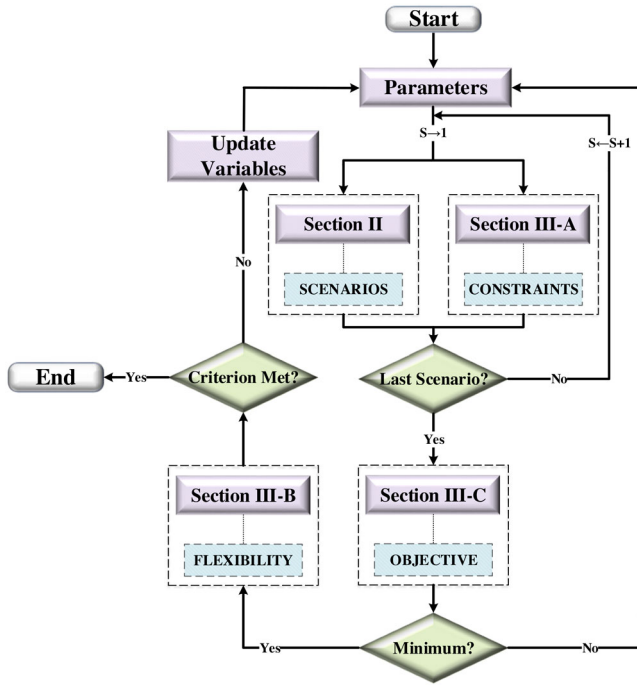
FIGURE 1 Flowchart of the proposed algorithm

ALGORITHM 1 Logic algorithm of solution methodology

1. **Start** →
2. **Input** data
3. **Set** parameters
4. **Set** scenarios
5. **while** true
   Solve (17)–(19)
6. **while** true
7. **for** $s \in S$
   $\min_s$(21) **s. t.**: (1)–(16)
   $s++1$
8. **if** (21) is minimum:
   Save (21)
   Break
9. **Check** (20)
10. **if** (20) is maximum:
   Save (20)
   Break
11. **← End**

newly installed transmission lines and BESS modules has been selected alongside Periodical options to minimize the total cost.

In the third loop, a new RES-BESS-based grid-scale system flexibility metric is measured to assess the impacts of BESS modules on the amount of system flexibility. In this regard, a computationally efficient offline fast mechanism is presented to repetitively calculate the system flexibility and deal with the specific amount of flexibility targets. To clarify, a novel repetitive approach is presented based on the investment budget to assess the price/benefit trade-off between minimizing the total cost against improving the system flexibility to finally find the best investment plan. Therefore, when the best option based on the first and second loops is detected, the amount of system flexibility is evaluated in an offline mode. Thus, if the amount of system flexibility is less than the specified limit, the system is concluded as an unacceptable condition in terms of the flexibility concept, which indicates that the system operator must add BESS modules to improve the system flexibility. As a result, by recognizing the vulnerable nodes, new constraints are added to the model to update the previous investment plan accordingly and as a result, increase the total cost. This method is repetitively continued until all investment options are checked to satisfy the specific system flexibility target. This approach is presented to converge the model faster alongside the fast-converged direct-optimization co-planning model; however, if multi-objective online optimization methods are used to measure power system flexibility, the model would converge at a slower pace. The algorithm is briefly presented as Algorithm 1.

To keep the security margin in this paper, it is assumed that the corresponding limits for the system flexibility can be securely 10% greater than the minimum desirable amount of the power system flexibility in the per-unit scale. Moreover, the

maximum number of available transmission lines to be installed and the available distributed BESS modules to be utilized are considered 3 and 12, respectively. Therefore, two binary variables are defined to measure the maximum number of installable transmission lines in each corridor. The location of installed transmission lines and BESS modules has been planned based on the optimization problem to minimize the total cost presented in the objective function. Assuming the worst-case scenario of demanded loads for the operational sub-problem, one set data of a sample summer day is picked.

5 | CASE STUDY

5.1 | Grid-scale test system

To optimally prove the efficiency of the proposed fast-converged direct-optimization co-planning algorithm in solving large-scale power systems, the proposed model is simulated on the modified version of the IEEE 73-bus test system. The case study includes 99 generating units, 117 transmission lines, and 51 load points. The network nodes and transmission lines data are taken from [13]. The investment cost of newly installed transmission lines is assumed to be 1,000 $/MVA-mile. Considering the real situation in this simulation, some wind farms are added to the case study including the generated multiple uncertainties scenarios. The data of wind farms peak generation and the 24-h

normalized pattern of wind farms generation are presented in Appendix A2. In this paper, we choose the lead-acid BESS (LABS) modules as an appropriate option for the applications of ESSs in large-scale power systems. Despite the commonness

TABLE 1 Investment results of case I

TOTAL INSTALLED TRANSMISSION LINES NUMBER = 39	
INSTALLED TRANSMISSION LINES (CORRIDOR NO./NUMBER)	(Corridor 3/1) (Corridor 6/1) (Corridor 10/1) (Corridor 11/2) (Corridor 21/3) (Corridor 23/1) (Corridor 28/1) (Corridor 43/1) (Corridor 50/1) (Corridor 51/2) (Corridor 60/3) (Corridor 61/1) (Corridor 66/2) (Corridor 80/1) (Corridor 82/1) (Corridor 83/2) (Corridor 88/2) (Corridor 90/1) (Corridor 97/3) (Corridor 98/3) (Corridor 103/2) (Corridor 115/3) (Corridor 117/1)
TOTAL INSTALLED BESS CAPACITIES = 2700 MW	
INSTALLED BESS CAPACITIES (NODE NO./CAPACITY)	(Node 3/50) (Node 5/50) (Node 6/150) (Node 8/200) (Node 11/150) (Node 14/400) (Node 16/50) (Node 28/100) (Node 29/250) (Node 30/100) (Node 34/150) (Node 38/150) (Node 50/300) (Node 51/100) (Node 54/50) (Node 62/400) (Node 65/50)

TABLE 2 Investment results of case II, III and IV

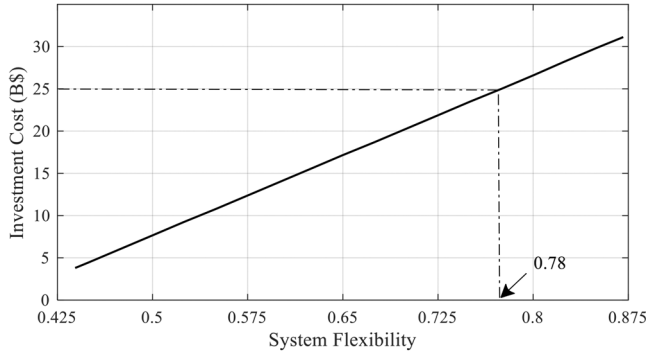| CASE II	Total added BESS capacities to Case I = 5700 MW
CASE III	Total added BESS capacities to Case II = 5200 MW
CASE IV	Total added BESS capacities to Case III = 5150 MW
ADDED BESS CAPACITIES TO CASE I (NODE NO./CAPACITY)	(Node 1/150) (Node 2/50) (Node 7/200) (Node 13/250) (Node 15/250) (Node 17/50) (Node 18/200) (Node 20/50) (Node 21/200) (Node 22/200) (Node 23/200) (Node 25/150) (Node 26/50) (Node 31/200) (Node 36/50) (Node 37/200) (Node 39/250) (Node 40/300) (Node 42/200) (Node 43/50) (Node 45/200) (Node 46/200) (Node 47/250) (Node 49/150) (Node 55/200) (Node 61/250) (Node 63/250) (Node 64/150) (Node 66/200) (Node 69/200) (Node 70/150) (Node 71/250)
ADDED BESS CAPACITIES TO CASE II (NODE NO./CAPACITY)	(Node 2/200) (Node 7/150) (Node 13/300) (Node 16/250) (Node 18/200) (Node 21/200) (Node 22/100) (Node 23/400) (Node 26/200) (Node 31/100) (Node 37/400) (Node 42/200) (Node 44/250) (Node 45/150) (Node 46/100) (Node 47/350) (Node 55/100) (Node 60/250) (Node 61/300) (Node 64/50) (Node 66/200) (Node 69/200) (Node 70/200) (Node 71/350)
ADDED BESS CAPACITIES TO CASE III (NODE NO./CAPACITY)	(Node 1/200) (Node 2/150) (Node 3/200) (Node 7/100) (Node 13/50) (Node 15/100) (Node 16/100) (Node 17/150) (Node 18/200) (Node 20/300) (Node 21/200) (Node 22/150) (Node 25/200) (Node 26/250) (Node 31/150) (Node 36/250) (Node 39/100) (Node 42/200) (Node 43/200) (Node 45/250) (Node 46/150) (Node 49/200) (Node 51/100) (Node 55/200) (Node 61/50) (Node 63/100) (Node 64/200) (Node 66/200) (Node 69/200) (Node 70/250)

of the proposed algorithm in applying all ESSs technologies, this type is applied due to its large capacity and higher efficacy. Note that the demanded loads and maximum capacity of generating units are multiplied by 2.2 to address the applicability of the proposed algorithm on the system flexibility as the original shape of the case study is highly reliable [48]. The MILP problem presented in this paper was solved via CPLEX solver on an Intel Xeon processor CPU @ 3.40 GHz with 16 GB RAM. The MILP gap for solving the problem is set to 0.1%; also, the average running time was 350 min.

6 | RESULTS

To better analyse the numerical results of our framework, four different cases are compared as follows:

I. Co-planning of TEP versus LABS modules without flexibility target.
II. Co-planning of TEP versus LABS modules with flexibility target equals 0.55.
III. Co-planning of TEP versus LABS modules with flexibility target equals 0.65.
IV. Co-planning of TEP versus LABS modules with flexibility target equals 0.75.

The results associated with the optimal investment plans for all cases are presented in Tables 1 and 2. The system cost results related to each case's optimal plans and RES-BESS-based grid-scale system flexibility are tabulated in Table 3. It can be traced that the number of newly installed transmission lines in all cases is 39, where corridors 21, 60, 97, 98, and 115 with the most installed transmission lines are the vulnerable corridors in the test system. As a result, to handle the congestion in transmission lines, the limit in installing new transmission lines should be increased, depending on the investment budget and geographical constraints. Moreover, it can be concluded that more LABS modules should be installed in the nodes near these corridors

TABLE 3 Investment results of Case II, III and IV

IC/OC (B$)	Case I	3.80/40.03
	Case II	10.79/120.60
	Case III	17.16/194.20
	Case IV	23.47/267.05
TC (B$)	Case I	40.59
	Case II	122.22
	Case III	196.75
	Case IV	270.45
System flexibility	Case I	0.439
	Case II	0.550
	Case III	0.650
	Case IV	0.750

to improve power system flexibility. Considering the flexibility target, Table 3 illustrates that the proposed co-planning model achieves an optimal expansion plan with flexibility criteria equal to 0.439, which cannot be regarded as a standard amount for the system flexibility mentioned in previous sections. Therefore, to increase the flexibility criteria of the optimal expansion plan, the installed LABS modules capacity must be increased, which is dependent on the investment budget.

It can be seen from the results of Case II, Case III, and Case IV that in order to achieve the flexibility target equal to 0.55,
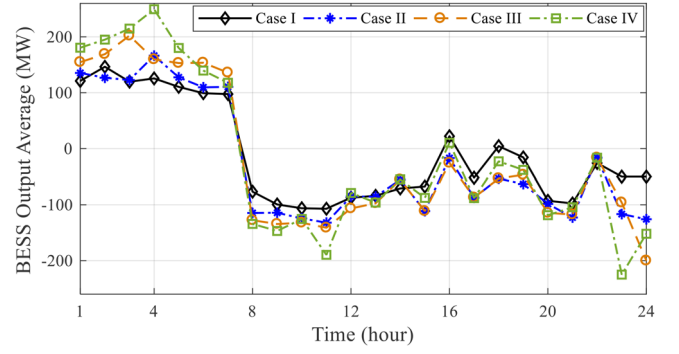
FIGURE 2 Investment cost based on system flexibility target

FIGURE 3 The average of hourly LABS modules' outputs as the difference between the charging and discharging powers

FIGURE 4 The average loading of available and installed transmission lines
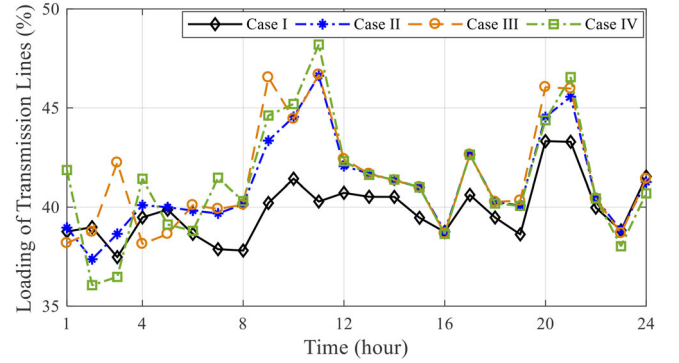
0.65, and 0.75 (increase up the system flexibility to 25%, 48%, and 71% compared to Case I), 5700 MW, 5200 MW, and 5150 MW capacity of the LABS modules should be added, respectively. In Periodical words, the capacity of newly installed LABS modules in Case I is 2700 MW; however, to reach the above-mentioned targets, we need to approximately install double capacity in each case. Therefore, improving the system flexibility results in a considerable increase in the total costs (increase the total cost to 81.63, 156.16, and 229.86 B$ compared to Case I). It should be noted that nodes 13, 18, 21, 23, 37, 42, 45, 47, 61, 66, 69, 70, and 71 are the most vulnerable nodes in the test system with the highest number of newly installed LABS modules (600 MW). Note that the limit on installing new LABS modules should be increased to improve the system flexibility to handle the total cost. The relationship between the system flexibility target and the total investment cost is discussed in Figure 2.

As a discussion, the important issue in installing these LABS modules is not only the total cost and flexibility target, but also the physical constraints such as installing in different weathers or applying for Periodical purposes alongside the flexibility which can be considered as critical constraints in future research works. This conclusion proves that the power system investors have tried to compromise the amount of power system flexibility to spend less on ESSs modules installation. Also, as known in power grids analysis, no system needs to be highly flexible and the desired amount of system flexibility depends on the systems' operators and owners. This is because although the flexibility target depends on the specific applications in power systems, a reasonable target of flexibility would be enough, generally for different research areas. As a result, the investment budget would play a vital role in each planning model. In doing so, by adding Figure 2, we have presented practical options for owners and investors to choose their flexibility target by considering their budget and managing their power system planning model based on these constraints.

It can be easily seen that the investment cost increases almost linearly as the system flexibility target increases. Moreover, by installing the supposed maximum capacity of the LABS modules in all nodes of the test system, the maximum value of the system flexibility can be 0.871 achieved by 31.12 B$ investment cost. Needless to say, to increase the maximum value of the system flexibility, the limited capacity of available LABS mod-

ules should be raised. In this practice, the maximum achievable amount of the system flexibility can be determined based on the available investment budget. As pointed out in the figure, by 25 B$ investment budget, the maximum achievable amount of the system flexibility is 0.78, which is completely plausible based on the standard amount of the system flexibility.

In the next step of the simulation, we precisely continue our analysis of the described cases from the viewpoint of the network's condition based on daily operation. In this regard, the outputs of installed LABS modules are depicted in Figure 3 as the difference between the charging and discharging powers in LABS modules ($P_{s,i,t}^{B+} - P_{s,i,t}^{B-}$). In the period of 1–7 AM, all LABS modules are charged due to the off-peak hours. Conversely, all modules are discharged in peak hours due to using power electricity. It should be noted that changing the BESS modules' statuses (between charging and discharging modes) depends on the amount of energy consumption and energy price in which the former has been managed daily based on Figure 3. Considering all cases, as easily predicted, the average hourly LABS modules scheduling in nodes increases by improving the system flexibility. In addition, the total loading of transmission lines in all cases is depicted in Figure 4 as a periodical viewpoint. As can be seen from this figure, the average loading of transmission lines occurs between 8 and 9 PM, when demands are high and LABS modules are discharged. This figure shows that Case II, Case III and Case IV have higher

as well as the same transmission loading compared to Case I since this loading scheme is required to smooth the generation and demands profile, which can prove the concept of the system flexibility. As a result, we have introduced a repetitive fast method to improve the RES-BESS-based grid-scale system flexibility by efficient LABS modules to smooth profiles in real applications. It has been proven that a considerable amount of investment is required to increase the amount of system flexibility.

7 | DISCUSSION

In this paper, unlike the previous research works, an MILP stochastic co-planning model of TEP versus BESS modules has been applied to improve power system flexibility by a novel RES-BESS-based grid-scale system flexibility metric. However, authors in [3] try to calculate the amount of flexibility without any scheme to improve it. Also, the repetitive fast offline method combined with a fast-converged optimization model is quite novel to reach the desired amount of flexibility in the lowest computational time which has not been addressed in previous research works. This method has helped us improve system flexibility without any computational complexity which can be efficiently applied in large-scale power systems. Moreover, we have considered the scenario-based stochastic multiple uncertainties along with the flexibility concept to make the model more realistic. In this paper, a module-type distributed BESS structure has been applied as ESSs technology to add a desirable amount of capacity with lower construction costs and no geographical constraints. Therefore, this model can prove that old-fashioned types of ESSs will be replaced in RES-based power grids by efficient BESS modules in the near future. From an economic point of view, the initial BESS investment cost is high. Still, it can be handled as incentive options in the planning part of the projects to investors who are seeking more flexibility for their power grids owing to the fact that the total cost can be reduced by using these modules which justify integrating distributed BESS in the future of power systems.

Future research works would focus on integrating different types of RESs in large-scale power systems. Then, the results of this paper can be compared to periodical types of RESs to effectively find out which resources would be more appropriate for different systems' situations. Moreover, periodical sources of uncertainties can be integrated with a correlation factor to model their exact impacts in each system. As our proposed model is fast-converged, novel optimization methods like data-driven distributionally robust TEP can be presented to develop an innovative decision-making platform. Also, this fast-converged method can be applied to measure the flexibility in an electricity market based on power system operational constraints in which changing the BESS modules' statuses can be predicted based on energy price.

On the periodical hand, by defining new mathematical prediction models such as machine learning applications in recent years, the presented results, such as candidate investment plans, transmission loadings, and hourly statuses of charging and dis-

charging would simply be predicted for subsequent years as initial data in new research works. So, these problems will be solved faster with more accuracy due to using precise results of the proposed model in this paper as initial values. It should be noted that the proposed flexibility method can be efficiently applied in distribution networks by considering the linearized AC power flow. Finally, by increasing the importance of power system resilient and the necessity to have more secure systems, this model can be applied in $N - k$ strategies to improve power system resilient as the proposed solution method is completely fast-converged which helps power system planners to add new computational complexity in actual power systems issues.

8 | CONCLUSION

In this paper, a fast-converged direct-optimization novel MILP model was presented to improve the system flexibility considering the impacts of Lead-Acid BESS technology on a linearized TEP framework. In this regard, a novel RES-BESS-based grid-scale system flexibility metric is suggested to hopefully achieve the desired system flexibility amount in numerical structure. Furthermore, considering the investment budget, a fast repetitive offline method is optimally proposed to reach the system flexibility target. The scenario-based stochastic multiple uncertainties associated with wind farms generation as well as demanded loads and also a new module-type distributed BESS structure for each node based on their efficiency are suggested to be more practical in the real environment, addressing previously TEP problems in the system flexibility and power system economics. The proposed model was applied to the modified IEEE 73-bus test system including wind farms. Techno-economic evaluation of the proposed analytics on the numerical results demonstrated the effectiveness of the LABS modules in improving system flexibility, investment plans, and power system economics. Note that a considerable amount of investment cost is required to increase the system flexibility that should be compromised or handled by incentive options.

NOMENCLATURE

Sets

T Set of hours, $t \in T$.
N Set of nodes, $i \in N$.
G Set of generating units, $g \in G$.
L Set of transmission lines, $l \in L$.
Ω Set of days in operational sub-problem, $\omega \in \Omega$.
S Set of multiple uncertainties scenarios, $s \in S$.

Parameters

C_l^L Vector of the investment cost of transmission lines, $C_l^L \in R^L$.
C_g^G Vector of operational cost of generating units, $C_g^G \in R^G$.
C^W Value of wind farms spillage cost.

$C^B/\hat{C}^B$ Power/energy investment cost of BESS modules.

C^F/C^V Fixed/variable maintenance cost.

P_{max}^B/E_{max}^B Maximum power/energy capacity of each BESS module.

$P_{s,i,t}^D/\Delta P_{s,i,t}^D$ 3-D matrix of demanded loads/subtraction of demanded loads between given time t and $t-1$, $P_{s,i,t}^D/\Delta P_{s,i,t}^D \in R^{S \times N \times T}$.

$P_{s,i,t}^W/\Delta P_{s,i,t}^W$ 3-D matrix of wind farms generation /subtraction of wind farms generation between given time $t-1$, $P_{s,i,t}^W/\Delta P_{s,i,t}^W \in R^{S \times N \times T}$.

$\Psi_{g,i}^G$ 2-D mapping matrix of generating units, $\Psi_{g,i}^G \in Z^{G \times N}$.

$\Psi_{l,i}^L$ 2-D mapping matrix of transmission lines (to-node branch minus from-node branch), $\Psi_{l,i}^L \in Z^{L \times N}$.

$P_{l,max}^L$ Vector of the maximum capacity of transmission lines, $P_{l,max}^L \in R^L$.

$P_{i,max}^W$ Vector of wind farms maximum generation, $P_{i,max}^W \in R^N$.

$P_{g,min}^G/P_{g,max}^G$ Vector of minimum/maximum capacity of generating units, $P_{g,min}^G/P_{g,max}^G \in R^G$.

ρ_s Vector of the probability of scenarios, $\rho_s \in R^S$.

β_l Vector of susceptance of transmission lines, $\beta_l \in R^L$.

$\delta_{i,max}$ Vector of maximum installable number of BESS modules, $\delta_{i,max} \in Z^N$.

π_1/π_2 Weight signals for normalizing the flexibility index.

σ_{min} The target for RES-BESS-based grid-scale system flexibility.

x/y Interest rate/lifetime in planning sub-problem.

$\Re$ Fixed coefficient in Big-M method.

η Efficiency of BESS modules.

Continuous Variables

TC Total cost.

IC/OC Investment/operational cost.

IC^L/IC^B Investment cost of installed transmission lines/BESS modules.

OC^G/OC^B Operational cost of generating units/BESS modules.

SC^W Wind farms spillage cost.

$\alpha'_l/\alpha''_l/\alpha'''_l$ Vector of $1^{st}/2^{nd}/3^{rd}$ installed transmission lines, $\alpha'_l/\alpha''_l/\alpha'''_l \in \{0,1\}^L$.

δ_i^B Vector of installed BESS modules, $\delta_i^B \in Z^N$.

$P_{i,max}$ Vector of maximum generating power, $P_{i,max} \in R^N$.

$\gamma_{s,i,t}$ 3-D matrix of flexibility index, $\gamma_{s,i,t} \in R^{S \times N \times T}$.

σ RES-BESS-based grid-scale system flexibility amount.

$P_{s,g,t}^G/\Delta P_{s,g,t}^G$ 3-D matrix of power of generating units/subtraction of power of generating units between given time t and $t-1$, $P_{s,g,t}^G/\Delta P_{s,g,t}^G \in R^{S \times G \times T}$.

$P_{s,i,t}^{B+}/\Delta P_{s,i,t}^{B+}$ 3-D matrix of BESS modules charging power/subtraction of BESS modules charging power between given time t and $t-1$, $P_{s,i,t}^{B+}/\Delta P_{s,i,t}^{B+} \in R^{S \times N \times T}$.

$P_{s,i,t}^{B-}/\Delta P_{s,i,t}^{B-}$ 3-D matrix of BESS modules discharging power/subtraction of BESS modules discharging power between given time t and $t-1$, $P_{s,i,t}^{B-}/\Delta P_{s,i,t}^{B-} \in R^{S \times N \times T}$.

$P_{s,i,t}^{ws}$ 3-D matrix of wind farms spillage power, $P_{s,i,t}^{ws} \in R^{S \times N \times T}$.

$E_{s,i,t}^B$ 3-D matrix of BESS modules' SoC, $E_{s,i,t}^B \in R^{S \times N \times T}$.

$F_{s,l,t}$ 3-D matrix of available transmission lines power flow, $F_{s,l,t} \in R^{S \times L \times T}$.

$F'_{s,l,t}/F''_{s,l,t}/F'''_{s,l,t}$ 3-D matrix of $1^{st}/2^{nd}/3^{rd}$ installed transmission lines power flow, $F'_{s,l,t}/F''_{s,l,t}/F'''_{s,l,t} \in R^{S \times L \times T}$.

$\Theta_{s,i,t}$ 3-D matrix of voltage phase angle, $\Theta_{s,i,t} \in R^{S \times N \times T}$.

DATA AVAILABILITY STATEMENT

Data sharing not applicable to this article as no datasets were generated or analysed during the current study.

ORCID

Hesam Mazaheri https://orcid.org/0000-0002-4115-5784

Sajjad Fattaheian-Dehkordi https://orcid.org/0000-0003-4770-7778

Moein Moeini-Aghtaie https://orcid.org/0000-0002-7656-6807

Mahmud Fotuhi-Firuzabad https://orcid.org/0000-0002-5507-9938

Matti Lehtonen https://orcid.org/0000-0002-9979-7333

REFERENCES

1. Cañas-Carretón, M., Carrión, M.: Generation capacity expansion considering reserve provision by wind power units. IEEE Trans. Power Syst. 35(6), 4564–4573 (2020)

2. Khasanov, M., Kamel, S., Rahmann, C., Hasanien, H.M., Al-Durra, A.: Optimal distributed generation and battery energy storage units

integration in distribution systems considering power generation uncertainty. IET Gener. Transm. Distrib. 15(24), 3400–3422 (2021)

3. Mazaheri, H., Moeini-Aghtaie, M., Fotuhi-Firuzabad, M., Dehghanian, P., Khoshjahan, M.: A linearized transmission expansion planning model under $N-1$ criterion for enhancing grid-scale system flexibility via compressed air energy storage integration. IET Gener. Transm. Distrib. 16(2), 208–218 (2022)

4. Cai, M., Yang, R., Zhang, X., Zhang, Y., Rahman, R.: Double-signal retail pricing scheme for acquiring operational flexibility from batteries. IEEE Trans. Sustainable Energy 13(2), 693–703 (2022)

5. Wang, L., Tao, Z., Zhu, L., Wang, X., Yin, C., Cong, H., Bi, R., Qi, X.: Optimal dispatch of integrated energy system considering integrated demand response resource trading. IET Gener. Transm. Distrib. 16(9), 1727–1742 (2022)

6. Chen, Y., Zhang, Z., Chen, H., Zheng, H.: Robust UC model based on multi-band uncertainty set considering the temporal correlation of wind/load prediction errors. IET Gener. Transm. Distrib. 14(2), 180–190 (2020)

7. Mazaheri, H., Ranjbar, H., Saber, H., Moeini-Aghtaie, M.: Expansion planning of transmission networks. In: Uncertainties in Modern Power Systems. pp. 35–56. Elsevier, Amsterdam (2020)

8. Hu, R., Li, Q.: Optimal operation of power systems with energy storage under uncertainty: A scenario based method with strategic sampling. IEEE Trans. Smart Grid 13(2), 1249–1260 (2022)

9. Khezri, R., Mahmoudi, A., Haque, M.: Impact of optimal sizing of wind turbine and battery energy storage for a grid-connected household with/without an electric vehicle. IEEE Trans. Ind. Inf. in press (2022)

10. Zhang, Z., Chen, Y., Liu, X., Wang, W.: Two-stage robust security-constrained unit commitment model considering time autocorrelation of wind/load prediction error and outage contingency probability of units. IEEE Access 7, 25398–25408 (2019)

11. Zhang, Z., Chen, Y., Ma, J., Liu, X., Wang, W.: Two-stage robust security constrained unit commitment considering the spatiotemporal correlation of uncertainty prediction error. IEEE Access 7, 22891–22901 (2019)

12. Connolly, D.: A review of energy storage technologies: For the integration of fluctuating renewable energy. Ph.D. Thesis. Limerick University (2010)

13. Saber, H., Heidarabadi, H., Moeini-Aghtaie, M., Farzin, H., Karimi, M.R.: Expansion planning studies of independent-locally operated battery energy storage systems (BESSs): A CVaR-based study. IEEE Trans. Sustainable Energy 11(4), 2109–2118 (2020)

14. Agarwal, A., Pileggi, L.: Large scale multi-period optimal power flow with energy storage systems using differential dynamic programming. IEEE Trans. Power Syst. 37(3), 1750–1759 (2022)

15. Sun, Y., Tian, Z., Wu, W., Du, Y., Wang, B., Xi, Y.: Iterative relaxation solution for AC optimal transmission network reconfiguration considering bus splitting. IET Gener. Transm. Distrib. 15(22), 3204–3214 (2021)

16. Dvorkin, Y., Fernandez-Blanco, R., Wang, Y., Xu, B., Kirschen, D.S., Pandžić, H., Watson, J.P., Silva-Monroy, C.A.: Co-planning of investments in transmission and merchant energy storage. IEEE Trans. Power Syst. 33(1), 245–256 (2018)

17. Wang, S., Geng, G., Jiang, Q.: Robust co-planning of energy storage and transmission line with mixed integer recourse. IEEE Trans. Power Syst. 34(6), 4728–4738 (2019)

18. Wong, L.A., Ramachandaramurthy, V.K., Walker, S.L., Ekanayake, J.B.: Optimal placement and sizing of battery energy storage system considering the duck curve phenomenon. IEEE Access 8, 197236–197248 (2020)

19. Rangel, S., Alberto, C., Canha, L.N., Sperandio, M., Miranda, V.: Mixed-integer stochastic evaluation of battery energy storage system integration strategies in distribution systems. IET Gener. Transm. Distrib. 16(4), 641–655 (2022)

20. Aguado, J.A., de la Torre, S., Triviño, A.: Battery energy storage systems in transmission network expansion planning. Electr. Power Syst. Res. 145, 63–72 (2017)

21. Qiu, T., Xu, B., Wang, Y., Dvorkin, Y., Kirschen, D.S.: Stochastic multistage coplanning of transmission expansion and energy storage. IEEE Trans. Power Syst. 32(1), 643–651 (2017)

22. Falugi, P., Konstantelos, I., Strbac, G.: Planning with multiple transmission and storage investment options under uncertainty: A nested decomposition approach. IEEE Trans. Power Syst. 33(4), 3559–3572 (2018)

23. Zhao, J., Zheng, T., Litvinov, E.: A unified framework for defining and measuring flexibility in power system. IEEE Trans. Power Syst. 31(1), 339–347 (2016)

24. Pourahmadi, F., Heidarabadi, H., Hosseini, S.H., Dehghanian, P.: Dynamic uncertainty set characterization for bulk power grid flexibility assessment. IEEE Syst. J. 14(1), 718–728 (2020)

25. Zhou, Z., He, C., Liu, T., Dong, X., Zhang, K., Dang, D., Chen, B.: Reliability-constrained AC power flow-based co-optimization planning of generation and transmission systems with uncertainties. IEEE Access 8, 194218–194227 (2020)

26. Ge, S., Xu, Z., Liu, H., Gu, C., Li, F.: Flexibility evaluation of active distribution networks considering probabilistic characteristics of uncertain variables. IET Gener. Transm. Distrib. 13(14), 3148–3157 (2019)

27. Silva, J., Sumaili, J., Bessa, R.J., Seca, L., Matos, M.A., Miranda, V., Caujolle, M., Goncer, B., Sebastian-Viana, M.: Estimating the active and reactive power flexibility area at the TSO-DSO interface. IEEE Trans. Power Syst. 33(5), 4741–4750 (2018)

28. Du, M., Huang, Y., Liu, J., Wu, G., Jawad, S.: CVaR-based generation expansion planning of cascaded hydro-photovoltaic-pumped storage system with uncertain solar power considering flexibility constraints. IET Gener. Transm. Distrib. 15(21), 2953–2966 (2021)

29. Riaz, S., Mancarella, P.: Modelling and characterisation of flexibility from distributed energy resources. IEEE Trans. Power Syst. 37(1), 38–50 (2022)

30. Ji, H., Wang, C., Li, P., Song, G., Yu, H., Wu, J.: Quantified analysis method for operational flexibility of active distribution networks with high penetration of distributed generators. Appl. Energy 239, 706–714 (2019)

31. Ma, J., Silva, V., Belhomme, R., Kirschen, D.S., Ochoa, L.F.: Evaluating and planning flexibility in sustainable power systems. IEEE Trans. Sustainable Energy 4(1), 200–209 (2013)

32. Wang, Z., Jochem, P., Fichtner, W.: A scenario-based stochastic optimization model for charging scheduling of electric vehicles under uncertainties of vehicle availability and charging demand. J. Cleaner Product. 254, 119886 (2020)

33. Saber, H., Mazaheri, H., Ranjbar, H., Moeini-Aghtaie, M., Lehtonen, M.: Utilization of in-pipe hydropower renewable energy technology and energy storage systems in mountainous distribution networks. Renewable Energy 172, 789–801 (2021)

34. Ranjbar, H., Hosseini, S.H., Zareipour, H.: Resiliency-oriented planning of transmission systems and distributed energy resources. IEEE Trans. Power Syst. 36(5), 4114–4125 (2021)

35. Trivedi, A., Aih, H.C., Srinivasan, D.: A stochastic cost–benefit analysis framework for allocating energy storage system in distribution network for load leveling. Appl. Energy 280, 115944 (2020)

36. Jithendranath, J., Das, D.: Stochastic planning of islanded microgrids with uncertain multi-energy demands and renewable generations. IET Renewable Power Gener. 14(19), 4179–4192 (2020)

37. Karki, R., Hu, P., Billinton, R.: A simplified wind power generation model for reliability evaluation. IEEE Trans. Energy Convers. 21(2), 533–540 (2006)

38. Farzin, H., Fotuhi-Firuzabad, M., Moeini-Aghtaie, M.: Stochastic energy management of microgrids during unscheduled islanding period. IEEE Trans. Ind. Inf. 13(3), 1079–1087 (2017)

39. Growe-Kuska, N., Heitsch, H., Romisch, W.: Scenario reduction and scenario tree construction for power management problems. In: IEEE Bologna Power Tech Conference Proceedings, pp. 23–26. Bologna, Italy (2003)

40. Mazaheri, H., Abbaspour, A., Fotuhi-Firuzabad, M., Moeini-Aghtaie, M., Farzin, H., Wang, F., Dehghanian, P.: An online method for MILP co-planning model of large-scale transmission expansion planning and energy storage systems considering N-1 criterion. IET Gener. Transm. Distrib. 15(4), 664–677 (2021)

41. Villumsen, J.C., Bronmo, G., Philpott, A.B.: Line capacity expansion and transmission switching in power systems with large-scale wind power. IEEE Trans. Power Syst. 28(2), 731–739 (2013)

42. Chen, B., Wang, J, Wang, L., He, Y., Wang, Z.: Robust optimization for transmission expansion planning: Minimax cost vs. minimax regret. IEEE Trans. Power Syst. 29(6), 3069–3077 (2014)

43. Cao, X., Wang, J., Zeng, B.: A study on the strong duality of second-order conic relaxation of AC optimal power flow in radial networks. IEEE Trans. Power Syst. 37(1), 443–455 (2022)

44. Huang, Y., Ai, X., Fang, J, Cui, S., Zhong, R., Yao, W., Wen, J.: Holomorphic embedding power flow algorithm for isolated ac microgrids with hierarchical control. IEEE Trans. Smart Grid 13(3), 1679–1690 (2022)

45. Homayoun, R., Bahmani-Firouzi, B., Niknam, T.: Multi-objective operation of distributed generations and thermal blocks in microgrids based on energy management system. IET Gener. Transm. Distrib. 15(9), 1451–1462 (2021)

46. Mazaheri, H., Khoshjahan, M., Moeini-Aghtaie, M., Fotuhi-Firuzabad, M.: Investigating the effects of ESS technologies on high wind-penetration power grids considering reliability indices. In: IEEE Texas Power Energy Conference, pp. 1–6. College Station, TX (2021)

47. Zhao, B., Conejo, A.J., Sioshansi, R.: Using electrical energy storage to mitigate natural gas-supply shortages. IEEE Trans. Power Syst. 33(6), 7076–7086 (2018)

48. Mazaheri, H., Abbaspour, A., Fotuhi-Firuzabad, M., Farzin, H., Moeini-Aghtaie, M.: Investigating the impacts of energy storage systems on transmission expansion planning. In: Iranian Conference on Electrical Engineering, pp. 1199–1203. Tehran, Iran (2017)

49. Grigg, C., Wong, P., Albrecht, P., Allan, R., Bhavaraju, M., Billinton, R., et al.: The IEEE reliability test system-1996. A report prepared by the reliability test system task force of the application of probability methods subcommittee. IEEE Trans. Power Syst. 14(3), 1010–1020 (1999)

APPENDIX

A1 | Linearization method

To describe our linearization method, the non-linear formulations have been presented as follows. As can be seen, the power flows in installed transmission lines constraints are non-linear due to multiplying the variables $\Theta_{s,i,t}$ and $\{\alpha'_l/\alpha''_l/\alpha'''_l\}$. In this vein, the well-known Big-M method is applied to linearize the DC optimal power flow formulations [40, 41]. Therefore, constraints (A1)–(A3) have been linearized as the linearized optimal power flows of installed transmission lines presented in (3)–(5).
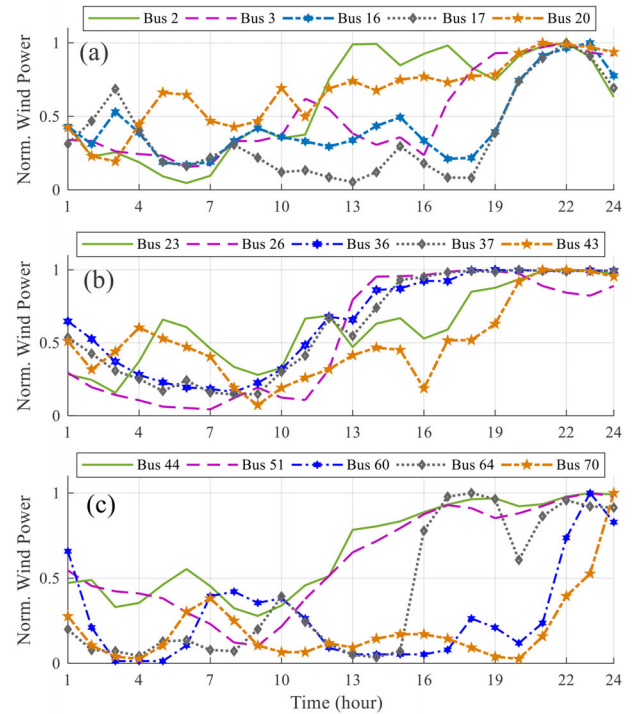
TABLE A1 Wind farms peak generation data

NODE NO.	CAPACITY (MW)	NODE NO.	CAPACITY (MW)
2	220	37	220
3	200	43	200
16	190	44	220
17	190	51	200
20	320	60	180
23	220	64	220
26	320	70	180
36	220	–	–

FIGURE A1 24-h normalized pattern of wind farms generation

A2 | RESs and BESS data

The data of wind farms' peak generation are presented in Table A1, while the 24-h normalized pattern of wind farms generation is shown in Figure A1 [13]. To model the uncertainty of wind power in this study, 50,000 scenarios are generated

$$F'_{s,l,t} + \Psi^L_{l,i}\beta_l\Theta_{s,i,t}\alpha'_l = 0: \quad \forall s \in S, l \in L, i \in N, t \in T \subseteq \left\{ \{0,1\}^L, R^L, Z^{L\times N}, R^{S\times L\times T}, R^{S\times N\times T} \right\} \tag{A1}$$

$$F''_{s,l,t} + \Psi^L_{l,i}\beta_l\Theta_{s,i,t}\alpha''_l = 0: \quad \forall s \in S, l \in L, i \in N, t \in T \subseteq \left\{ \{0,1\}^L, R^L, Z^{L\times N}, R^{S\times L\times T}, R^{S\times N\times T} \right\} \tag{A2}$$

$$F'''_{s,l,t} + \Psi^L_{l,i}\beta_l\Theta_{s,i,t}\alpha'''_l = 0: \quad \forall s \in S, l \in L, i \in N, t \in T \subseteq \left\{ \{0,1\}^L, R^L, Z^{L\times N}, R^{S\times L\times T}, R^{S\times N\times T} \right\} \tag{A3}$$

and then, the generated scenarios are decreased to an appropriate number to make the problem solvable (30 scenarios). The value of wind farms spillage cost is supposed to be 200 $/MWh [13] and the 24-h demands pattern is derived from [49] for a one-sample summer day to consider the worst-case scenario. The estimated power and energy costs of LABS modules are bounded into 200–580 $/kW and 225–300 $/kWh, respectively [12]. In this paper, 225 $/kW and 250 $/kWh are considered as the power and energy investment costs for each LABS module. Also, the estimated fixed and variable maintenance costs are considered to be 1.55 $/kW-year and 0, respectively. The power and energy capacities of each LABS module are supposed to be 50 MW and 200 MWh and as a result, the maximum installable capacity of the LABS modules is assumed to be 600 MW (12 × 50 MW) in each node. The initial SoC value of the LABS modules is supposed to be 0 at midnight. Finally, the annual interest rate is supposed to be 0.12 in a 10-year lifetime.